Biological Impacts of Hydraulic Disturbances Associated with Jet Boating on the Chilkat River, Alaska

D.F. Hill[1], B.D. Younkin
Department of Civil & Environmental Engineering
The Pennsylvania State University
University Park, PA 16802

January 2005

[1]Contact: 814.863.7305, dfh@engr.psu.edu

Contents

List of Figures

List of Tables

Conversion Factors

Every effort is made in this report to use the SI (metric) system of units. The following table of conversions will assist those wishing to convert reported values in SI units to BG units.

Quantity	Multiply	by	To Obtain
Area	square meter	10.77	square foot
Area	square kilometer	0.386	square mile
Area	square kilometer	247.1	acre
Energy	joules	0.738	foot pounds
Flow Rate	cubic meters per second	35.31	cubic feet per second
Flow Rate	cubic meters per second	15,850	gallons per minute
Length	meter	3.281	foot
Length	kilometer	0.622	mile
Mass	kilograms	0.685	slugs
Mass	kilograms	2.21	pounds mass
Power	watts	0.00134	horsepower
Power	watts	0.738	foot pounds per second
Speed	meters per second	2.237	miles per hour
Stress / Pressure	Pascals	0.000145	pounds per square inch

Nomenclature

The following lists and defines the variables that are used herein. Note that, in a few cases, a single symbol is used to denote multiple quantities. Every effort is made to clarify this in the text of the report.

Symbol	Description
A	area
C	concentration
d_{50}	median grain size diameter
Φ	dissipation of energy
g	gravitational acceleration
γ	fluid specific weight
h	depth
h_L	head loss
k	turbulent kinetic energy
K_L	loss coefficient
K_y	diffusion coefficient
$\dot{m}$	mass flow rate
μ	absolute viscosity
P	power
Q	discharge
ρ	fluid density
τ_0	bank / bed shear stress
(u, v, w)	velocity components
u_*	shear velocity
V	velocity
$\overline{V}$	mean velocity
V'	fluctuating velocity
$\mathcal{V}$	volume
(x, y, z)	spatial coordinates

Preface

The work described in this report was conducted for the Alaska Department of Fish and Game (ADFG), Sport Fish Division.

The field work was performed during June of 2003 by researchers from the Department of Civil and Environmental Engineering at the Pennsylvania State University. Assistance with logistical details was provided by members of ADFG. The laboratory work was performed during the winter and spring of 2004 by researchers from the Department of Civil and Environmental Engineering and the School of Forest Resources at the Pennsylvania State University. Assistance with the laboratory experiments was provided by Tim Stecko, Doug Fischer, and Justin Koller.

The authors wish to thank ADFG for providing many of the on-site resources required for the field study.

Summary

A two-part study has been conducted in an effort to understand the impacts, if any, that commercial jet boating is having on rearing juvenile salmonids in the upper Chilkat River, Alaska. In the first part of the study, measurements of near-bank fluid velocity and turbidity were made. The measurements were made at a variety of depths and distances from the bank in an effort to build up a complete picture of the hydraulic climate in the near-bank region. The goal of this component of the study was to determine the ambient characteristics typical of rearing habitat.

In the second part of the study, controlled laboratory experiments investigating the biological response of salmon fry to varying levels of these hydraulic disturbances were conducted. The goal of this component of the study was to determine whether or not salmon fry respond negatively to the elevated hydraulic disturbances that are associated with boat wakes breaking on the banks of the river.

Some of the key findings of this study include:

- Ongoing erosion pin measurements in the Chilkat River (since summer 2002) demonstrate steady erosion of the banks in response the the loadings on the banks. These loadings include the stream flow and the impacts of boat wakes. For the most part, larger erosion values are found in larger channels, but there are some exceptions to this generalization.

- Numerous estimation methods applied to the field data arrived at a shear velocity of $5 - 10$ cm s^{-1} in the vicinity of the banks. This parameter is of broad use in terms of characterizing the mean and turbulent flow fields.

- Field measurements consistently placed the ambient, or background, turbidity of the river at ~ 100 NTUs (nephelometric turbidity units).

- Laboratory trials revealed that the presence of fluid turbulence reduced the growth rate of salmon fry when compared to a control group exposed to no turbulence. However, the reduction in growth rate appeared not to be a function of the turbulence level in the tank.

- Laboratory trials revealed that the presence of turbidity did not seem to affect the growth rate of salmon fry. Moreover, the growth rate did

not appear to be function of the turbidity level in the tank.

Chapter 1

Introduction

1.1 Historical Overview of the Chilkat River Basin

The Chilkat River basin, consisting of the Chilkat, Klehini, Tsirku, and Kelsall Rivers, lies approximately 80 miles northwest of Juneau, Alaska, and drains into the upper Lynn Canal. A significant portion of the basin overlaps with the 49,000 acre Chilkat Bald Eagle Preserve (CBEP). The preserve was designated by the State Legislature in 1982. Prior to this, the importance of the large fall / winter gatherings of bald eagles was recognized through the designation of a 4800 acre Critical Habitat Area in 1973 and the adoption of the Haines / Skagway Land Use Plan in 1979.

As described in Alaska statute, and as reviewed by the Alaska Department of Natural Resources (ADNR, 2002), the CBEP was created to:

- Protect and perpetuate the Chilkat bald eagles and their essential habitats within the preserve,
- Protect and sustain the natural salmon spawning and rearing areas of the Chilkat River and Chilkoot River systems in perpetuity,
- Provide continued opportunities for research, study, and enjoyment of bald eagles and other wildlife,
- Maintain water quality and necessary water quality,

- Provide for the continued traditional and natural resource based lifestyle of the people living in the area, and
- Provide for other public uses consistent with the primary purpose of the Preserve.

In 1985, a plan for managing the Preserve was adopted. During the period of 2001-2002, a revision process for the plan was undertaken. One of the issues of concern, and the one pertinent to the present study and report, is that the Preserve has experienced greatly increasing levels of commercial recreational use over the past 10 years. The specific commercial use of relevance to the present study is that of large-scale jet-boat tours of the upper Chilkat River, between Wells Bridge and the confluence with the Kelsall River.

1.2 Review of Findings from the 2002 Study

Concern that operation of these large jet-boats was having an impact on salmon habitat prompted the ADFG to sponsor a field project in the summer of 2002 (Hill *et al.*, 2002). The main objective of that study was to measure the near-bank hydraulic parameters associated with jet-boating activity. These parameters included wake heights and turbidity levels.

The results of that study indicated that the boat wakes generated by commercial traffic were capable of dislodging sediment from the banks of the river. Peak values of recorded near-bank turbidity were found to far outweigh (by an order of magnitude) the ambient load of the river and were found to be an increasing function of wake height.

Comparisons of estimates of parameters such as shear stress, energy, and power suggested that, in some channels, the loading associated with boat wakes could exceed that of the streamflow. An equation relating wake height to 'sailing line' distance was developed in an effort to provide guidelines for minimizing the impacts of boat wakes on the river banks.

In conclusion, the 2002 field study demonstrated that, despite the relatively low usage levels on the Chilkat River, the potential impacts associated with boating could not be ruled out.

1.3 Study Scope and Limitations

The goal of the present field and laboratory study has been to investigate the consequences, if any, of these hydraulic loadings on juvenile salmon. ADFG biologists have documented near-bank areas as being productive rearing habitat. These areas, where wakes shoal, break, and dislodge sediment are those most heavily impacted by boating activity.

The specific goals of the field study were to (i) revisit numerous sites where erosion pins were placed during the 2002 field season and to (ii) obtain data on the distribution of velocity (both mean and turbulent) and turbidity in numerous near-bank areas.

The specific goals of the laboratory study were to determine how juvenile coho salmon respond to increasing levels of turbulence and turbidity. While it is of course impossible to replicate the exact field situation in a laboratory setting, efforts have been made to reproduce certain elements, such as the intermittent and relatively short-duration nature of the loading associated with boating activity. In addition, native sediments have been brought back from the Chilkat River in order to provide the turbidity for the present trials. To gauge whether or not any systematic trend exists, a control group and three treatment groups (each at a different loading level) were used for the laboratory study.

1.4 Report Outline

A brief review of near-bank hydraulics, along with an extensive review of the biological response of fish to hydraulic stresses, is presented in Chapter 2. Chapter 3 describes the field experiments and Chapter 4 describes the laboratory experiments. Finally, Chapter 5 provides discussion of the results, conclusions, and a discussion of any additional work that should be done.

Chapter 2

Review

In this chapter, previous studies dealing with the biological impacts of turbulence and turbidity on juvenile fish are breifly reviewed.

2.1 Hydrodynamic Imapcts

First of all, it is worth discussing what exactly constitutes a hydrodynamic impact. From a lay point of view, there is certainly the notion that impact is in some way associated with, and proportional to, the *flow* of water. However, it is not quite so simple. Fluid velocity, in and of itself, is not an indicator of a stressful environment. In the case of a fluid flow that is spatially uniform and temporally steady, there will be no sensation of motion at all.

There are two basic mechanisms that can lead to a fluid flow exerting a 'load' on an object that is being carried along by the flow. First of all, and as illustrated in Fig. 2.1, in a flow that is steady in time, but that has spatial variations in velocity, there are *gradients* in velocity present. These gradients are significant in that, for an object of some finite size, the fluid velocity along one edge of the object may differ from that along another edge. These different velocities result in a shear stress which, in turn, seeks to impart rotational motion to the object. This rotational motion can lead to accelerations of a damaging magnitude.

The other basic mechanism, as illustrated in Fig. 2.2, is associated with the temporal variations of a fluid flow and is therefore, by definition, associated with the turbulent nature of a fluid flow. Here, although the velocity may not vary significantly between closely adjoining points in space (the ve-

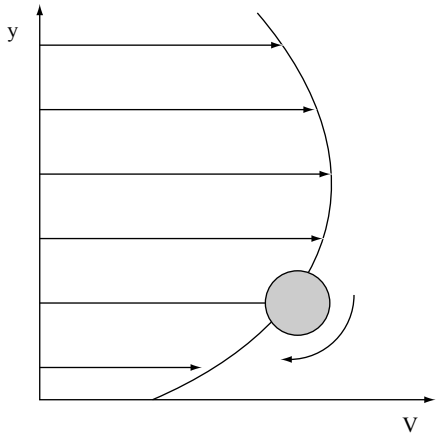

Figure 2.1: Schematic of rotational motion imparted by the spatial variation of mean velocity.

locity *gradients* are small), the velocity can, at a single point, fluctuate wildly in time. As shown in the figure, the velocity $V(t)$ recorded at some point in space is a function of time. By sampling over a long interval, T, it is possible to compute the time-averaged, or *mean* velocity;

$$\overline{V} = \frac{1}{T}\int_{t=0}^{t=T} V\ dt.$$

Thus, at any instant in time, the velocity is given by the sum of the mean velocity and the 'fluctuating' velocity, i.e. $V(t) = \overline{V} + V'$.

Now, the time-average of V' itself is, by definition, equal to zero and, therefore, not very useful. The root mean square value of the fluctuation, however, given by

$$V'_{\text{rms}} = \left(\frac{1}{T}\int_{t=0}^{t=T} V'^2\ dt\right)^{1/2},$$

is, in general, non-zero and a very useful measure of how turbulent the flow is. In particular, the ratio of the rms value of a velocity component to its mean value is referred to as the turbulence intensity. A flow that has a high turbulence intensity experiences significant accelerations that, as with the case of accelerations due to shear-induced rotation, can be damaging.

Morgan *et al.* (1976) studied the effects of shear stress on fish eggs and larvae, specifically bass and perch. They used a system that consisted of

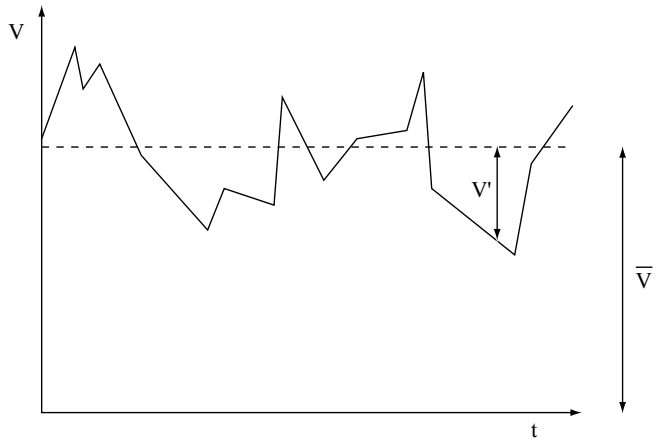

Figure 2.2: Schematic of a turbulent velocity signal.

two concentric cylinders, one of which was rotating, the other of which was fixed. In principle, the shear stress inside the annulus between the cylinders is a function of the cylinder diameters, rotation rate, and fluid properties, and can therefore be systematically varied. Batches of eggs were subjected to long-term (2-3 day) exposure and a regression equation between mortality and shear stress was developed. While of value in terms of its effort to systematically investigate these effects in the laboratory, the authors inappropriately applied a laminar theory to the case of a turbulent flow.

Killgore *et al.* (1987) studied the effects of turbulence on the yolk-sac larvae of paddlefish. This was accomplished by recirculating water, at either low or high rates, through circular raceways. This hydrodynamic 'loading' was done in an intermittent fashion. Unfortunately, this study also had some problems, from a fluid mechanical point of view. While the authors repeatedly referred to levels of 'turbulence,' their manuscript gave levels of shear stress. Therefore, it is not entirely clear *what* parameter was being systematically varied.

Sutherland & Ogle (1975) conducted a lab study on the effects of jet boats on salmon eggs. Initially, field experiments were performed by operating jet boat over pressure sensors buried in gravel beds. The observed pressure gradients were later reproduced in a laboratory setting where gravel and salmon eggs were packed into a vertical column. The eggs were exposed to the loading for a time period on the order of one minute. After an individual

test, the fatality rate was measured. Tests were performed on eggs of different 'ages,' from 6 to 13 days and fatalities averaged about 40 percent.

Much more recently, a report by Neitzel *et al.* (1998) discusses the exposure of small (5-10 cm) fish to extremely high-level, short-duration bursts of shear stress. The main motivation for this work had to do with fish passage through hydroelectric turbines. The high-stress environment was created with a high-velocity water jet, discharging into an ambient body of water. The fish were injected into the 'edge' of this jet through a small feeder tube. The biological stress on the fish was measured by subsequently inspecting the fish for death and significant injury. Many different species (e.g. salmon, trout, shad, etc.) were studied and it was found that there was not very much variation in response among the species.

Finally, a study by Rehmann *et al.* (2003) studied the effects of fluid turbulence on the mortality of zebra mussel larvae. From a fluid mechanical point of view, this study was very well done. An acoustic doppler velocimeter was used to characterize the velocity field induced by a bubble plume in a tank. The frequency spectra of the time series of the velocity data were then fit to the theoretical Batchelor spectrum allowing for the estimation of the dissipation of turbulent kinetic energy. This, in turn, allowed for the estimation of the Kolmogorov scale, which is the scale of the smallest turbulent eddies in the flow. It was found that the greatest mortality occurred when the larvae were approximately equal in size to this scale.

2.2 Turbidity Impacts

Gregg & Bergersen (1980) studied the effects of turbidity (and turbulence, incidentally) on Mysis relicta (opossum shrimp). Three turbidity and four turbulence levels were considered, for a total of 12 trials. As with some of the previously mentioned studies, the way in which the authors defined 'turbulence' was unsound. After initiating the experiment, mysids were examined on days 2, 4, 6, and 8 in order to determine mortality. The results indicated that turbidity was not that important in contributing to mortality.

Morgan *et al.* (1983) considered the effects of sediment on the eggs and larvae of bass and perch. The study found that percent hatch was not significantly affected by suspended sediment concentration levels up to about 5 grams per liter, but that developmental rates were severely lowered at concentrations above 1.5 grams per liter. Larvae showed significant mortality

when exposed to 24 and 48 hour durations of high turbidity. Arruda *et al.* (1983) studied the effects of turbidity on zooplankton and showed that modest levels severely reduced feeding rates. Finally, Breitburg (1988) studied the effects of turbidity on prey consumption by striped bass larvae. These were very short-duration (half hour) experiments. Tanks of different turbidity levels were set up and it was found that high turbidity levels reduced the number of copepods captured by the larvae.

Turning attention to the effects of turbidity on fish at a more advanced developmental stage, an excellent review is provided by Bash *et al.* (2001). First, the authors discuss how effects can be categorized as lethal, sub-lethal, and behavioral. Also, they discuss how duration of exposure, frequency of exposure, level of exposure, and life stage of the fish all play a significant role. They review laboratory studies that detailed gill trauma, elevated blood sugars, and elevated plasma glucose (Servizi & Martens, 1987), as well as reduced growth rates (Sigler *et al.*, 1984). Regarding the growth rates, the work by Sigler *et al.* (1984) showed that turbidities as low as 25 NTUs (NTU - nephelometric turbidity unit) reduced growth.

Moving on to behavioral effects, Sigler *et al.* (1984) showed that fish would migrate away from regions of relatively high turbidity (~ 150 NTUs) to regions of relatively low turbidity (~ 60 NTUs). Newly emerged fry were shown to be even more susceptible. Berg (1982) showed that streams affected by frequent short-term sediment pulses with concomitant loss of territoriality may experience a decrease in growth and feeding rates. Berg & Northcote (1985) showed that, during turbid phases ($\sim 30-60$ NTUs), territories broke down and subordinate fish captured a greater proportion of the prey. Other studies (Berg, 1982) have shown that fairly low turbidity levels ($\sim 20-60$ NTUs) caused fish to mis-strike prey items. Another issue (Newcombe & MacDonald, 1991) is that increased turbidity levels may affect the benthic community and therefore decrease the food supply.

Bash *et al.* (2001) also reviewed the current state and provincial turbidity standards for the Pacific Northwest, British Columbia, and Alaska. For Alaska, the standard is 25 NTUs above natural condition. Note that this standard is an 'end-of-pipe' standard, unless a mixing zone has been approved.

Chapter 3

Field Study

The Chilkat River Basin is illustrated in Figs. 3.1-3.4. Basic hydrologic information on the basin is provided by Bugliosi (1985) and is reviewed by Hill *et al.* (2002). The work in both the 2002 and the 2003 field seasons took place in the upper basin, above Wells Bridge. Figure 3.5 presents a mosaic of aerial photographs of the upper basin. In addition, key reference locations are noted on this figure. Throughout much of the rest of this chapter, reference will be made to many of the sites listed.

3.1 Erosion Pin Sites and Data

An erosion pin is a simple, yet effective, way to measure the amount of erosion that occurs at a given location. A pin is nothing more than a thin and long metal rod that is driven perpendicularly into the surface (river bank, river bed, etc.) of interest. By measuring, at an initial time and then some subsequent time, the length of the pin that is exposed, the amount of erosion that occurred between the two times is immediately determined.

During the 2002 field experiment, pins were placed at a number of locations. At each location, three pins were placed. All pins were $\sim$ 1 cm diameter rebar and were driven approximately 1 m into the bank, leaving approximately 15 cm initially exposed. Of the three pins, one was placed at the current level of the water, the second was placed 15 cm vertically above, and the third was placed 15 cm vertically below. All pins were placed in June. The pin locations, including GPS waypoints where available, are given by:

1. **LC1** (N 59.29.269 W 136.03.652) - This lies above the Kelsall boat launch in the 'left' (looking upstream) channel. Pins were placed in both the west and east banks of the channel.

2. **LC2** (N 59.29.006 W 136.03.208) - This lies approximately halfway between **LC1** and the boat launch. Pins were placed in both the west and east banks of the channel. The west pins are slightly upstream of a large culvert.

3. **MC1** - This is a site near the southern end of what is referred to as Dry Lake. This is in the 'middle' channel above the boat launch. Pins were placed in the west bank only.

4. **SHEEP CYN** (N 59.27.948 W 135.59.245) - This location is about three fourths of the way up the small clearwater channel leading into Sheep Canyon Lake. Pins were placed in both the west and east banks of the channel.

5. **EAST CHAN** (N 59.25.605 W 135.55.828) - This is in the east channel, not too far above Wells Bridge. Pins were placed in both the west and east banks.

6. **EC 2** - This location is in the east channel, in between **EAST CHAN** and **SHEEP CYN**. Pins were placed at two locations in the west bank only. The lower set is slightly above the 'tip' of the island; the upper set is approximately 30 meters north of the lower set.

7. **MC3 EAST** (N. 59.29.025 W 136.02.932) This location is approximately halfway between the Kelsall boat launch and Dry Lake. It is just above a 'point' separating this middle channel from a very small tributary on the right.

8. **MC3 WEST** (N 59.28.990 W 136.02.986) - This location lies more or less directly across the channel from **MC3 EAST**.

9. **KELSALL** - This location is on the west bank of the main channel, slightly upstream of what is referred to as Jacquot's Landing and slightly downstream of the confluence of the Chilkat and Kelsall Rivers.

During the 2003 field experiment, all pin locations were revisited and the erosion amounts were recorded. These erosion amounts are summarized in Table 3.1.

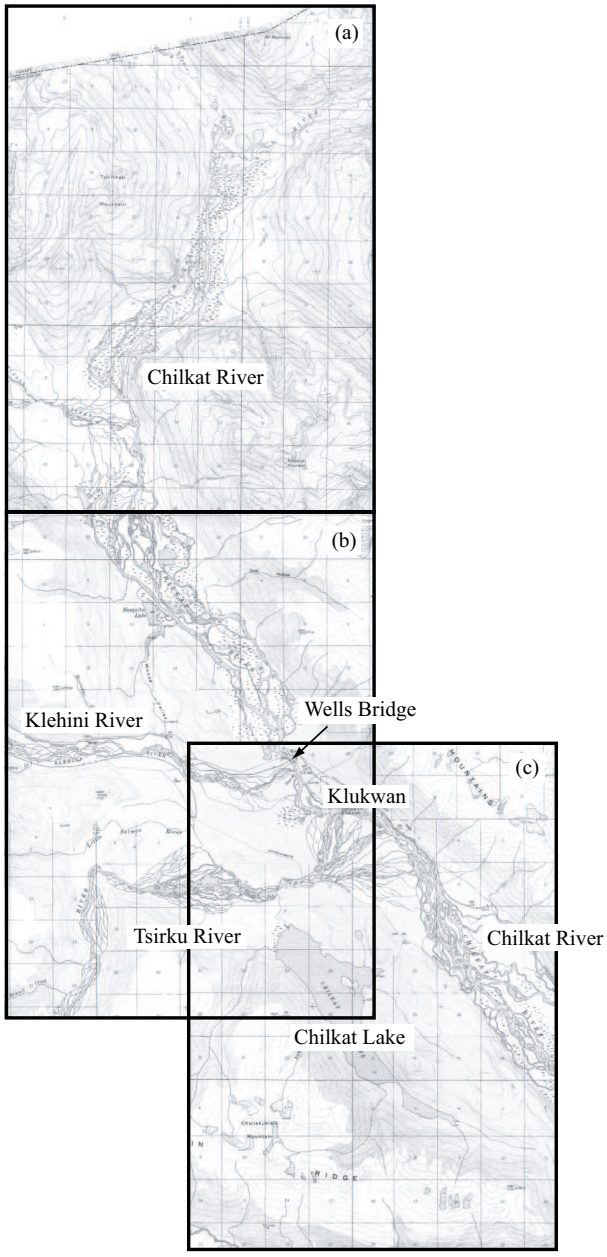

Figure 3.1: Topographic view of the Chilkat River basin. Source: USGS 7.5 minute Skagway B-3 & C-3 quadrangles.

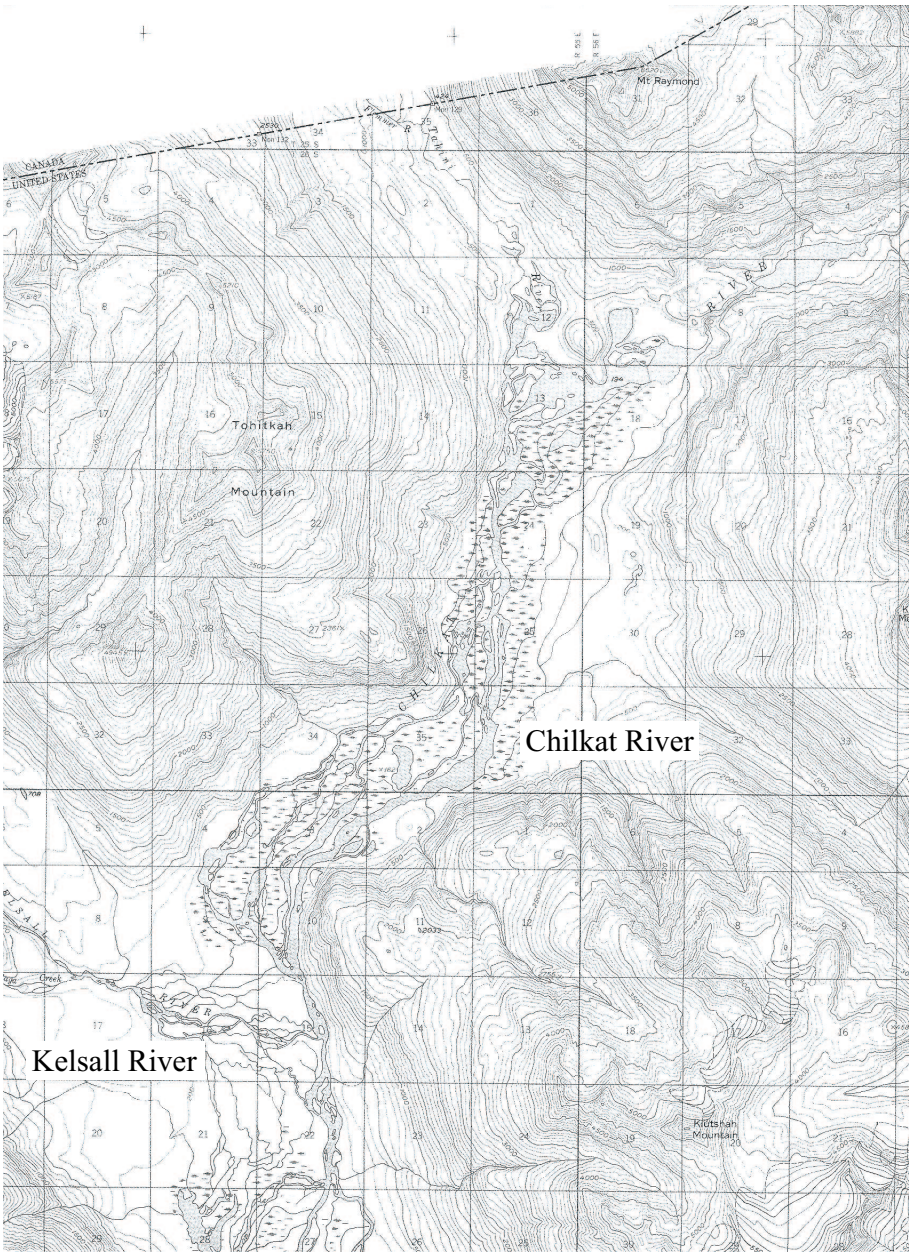

Figure 3.2: Topographic closeup view of region (a) from Fig. 3.1. Source: USGS 7.5 minute Skagway B-3 & C-3 quadrangles.

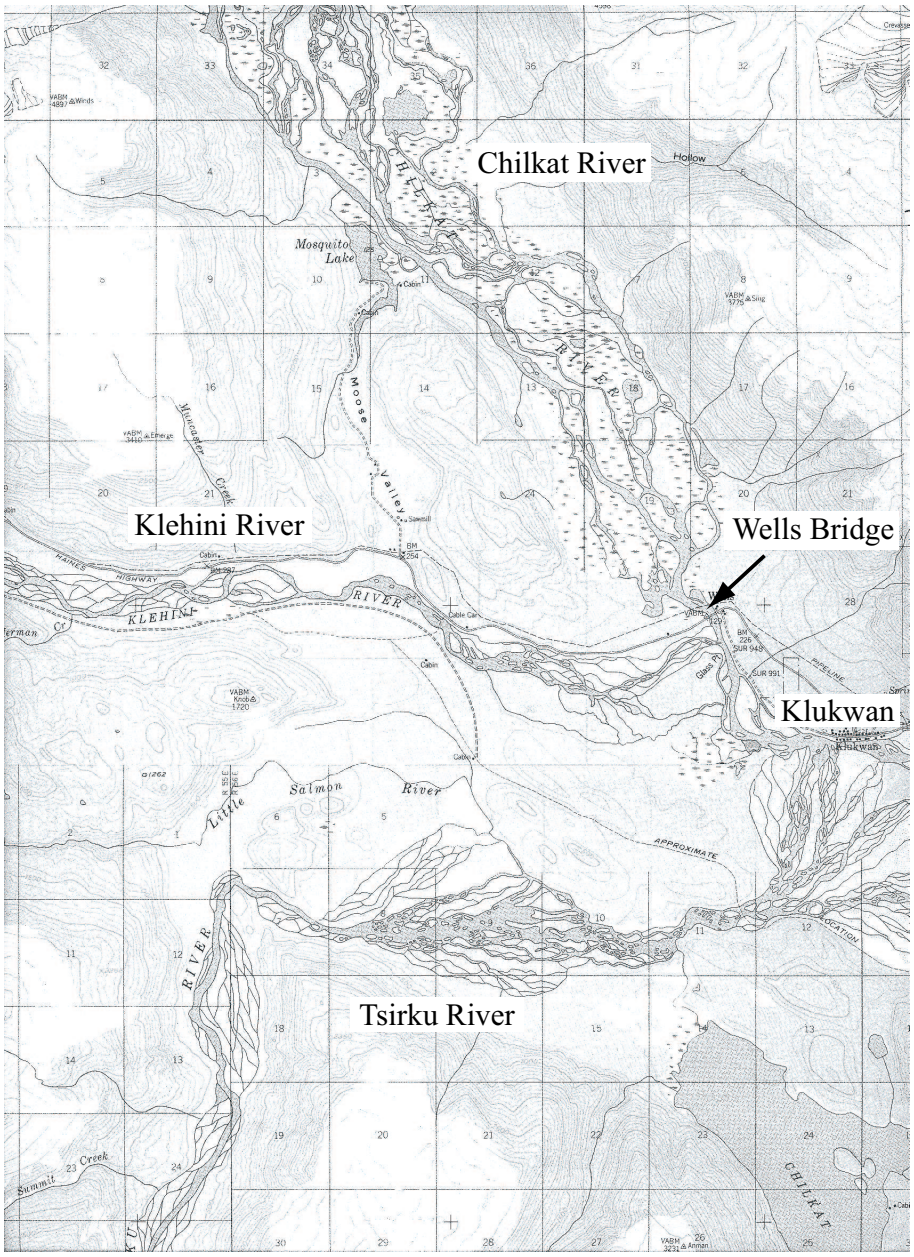

Figure 3.3: Topographic closeup view of region (b) from Fig. 3.1. Source: USGS 7.5 minute Skagway B-3 & C-3 quadrangles.

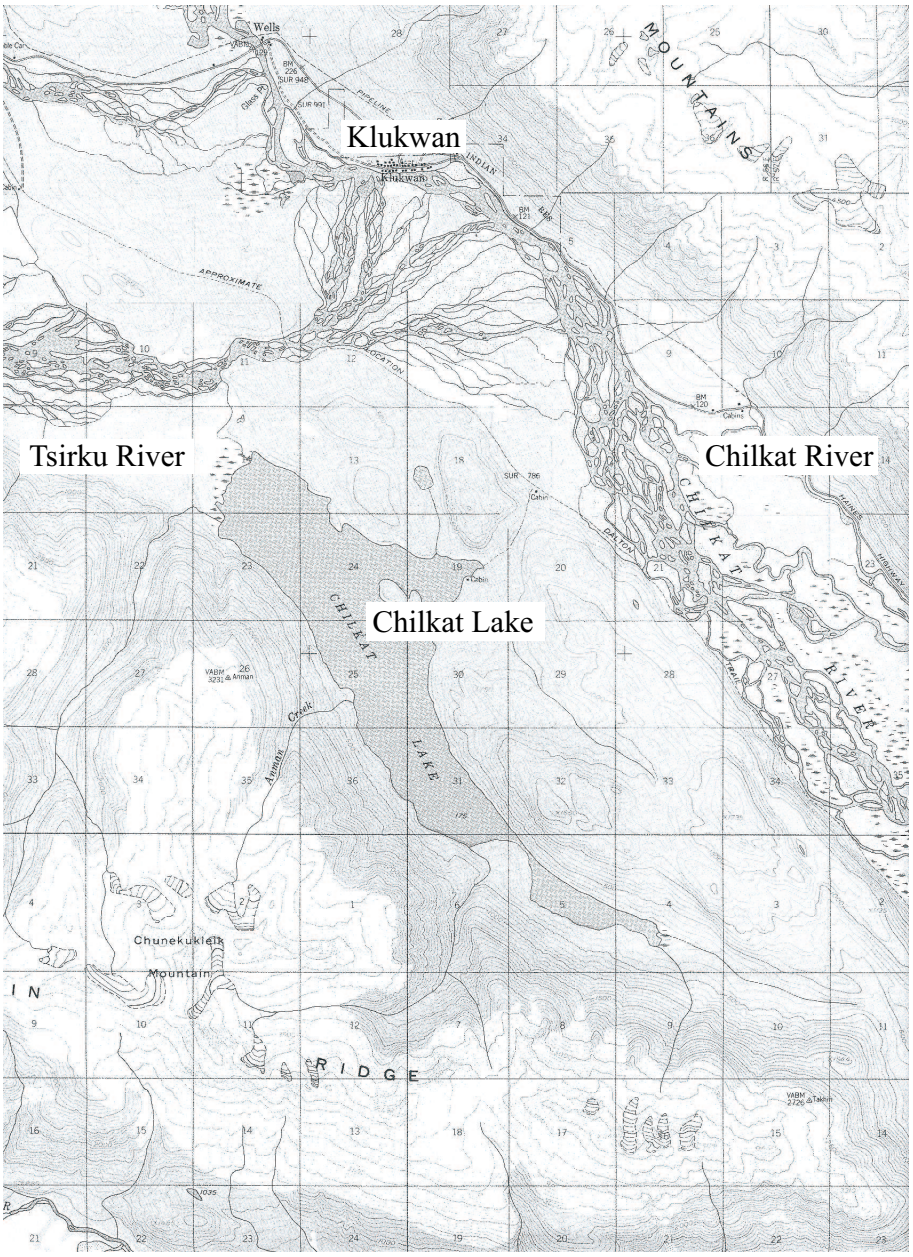

Figure 3.4: Topographic closeup view of region (c) from Fig. 3.1. Source: USGS 7.5 minute Skagway B-3 & C-3 quadrangles.

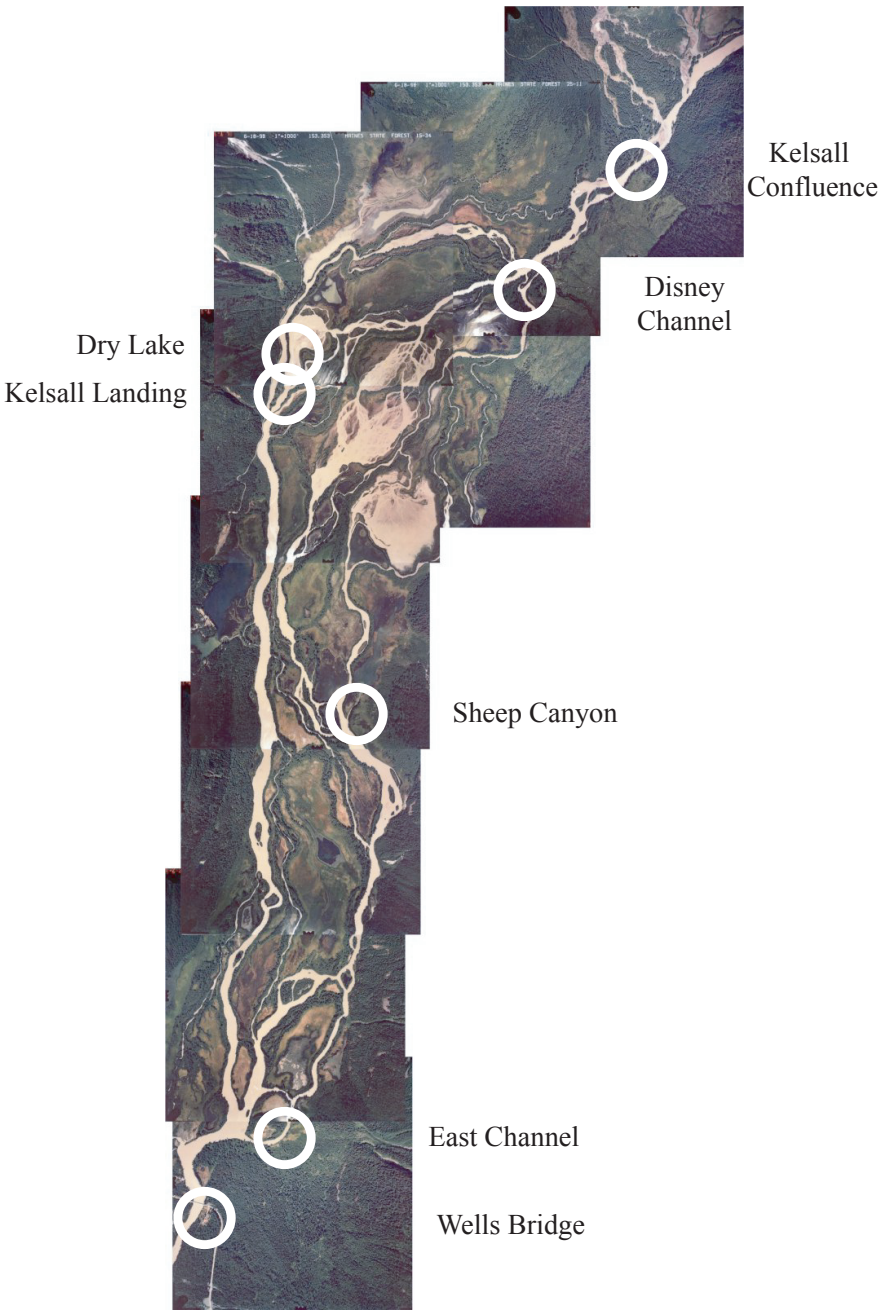

Figure 3.5: Aerial photograph mosaic indicating several reference locations in the Upper Chilkat Basin.

Location	Notes	Upper Pin (cm)	Middle Pin (cm)	Lower Pin (cm)	Average (cm)
LC1	West bank	2.5	0	0	0.8
	East bank	2.5	7.5	2.5	4.2
LC2	West bank	0	0	0	0
	East bank	0	0	0	0
MC1		35.5	35.5	35.5	35.5
SHEEP CYN	West bank	20.3	12.7	10.2	14.4
	East bank	0	7.6	7.6	5.1
EAST CHAN	West bank	10.2	2.5	2.5	5.1
	East bank	0	0	2.5	0.8
MC3 EAST		35.5	35.5	35.5	35.5
MC3 WEST		30.4	45.7	27.9	34.7
EC2	Upstream location	5.1	5.1	5.1	5.1
EC2	Downstream location	7.6	7.6	0	5.1
KELSALL		Missing[1]	Missing	Missing	n/a

Table 3.1: Erosion pin data for the Upper Chilkat River. Values given reflect the amount of erosion observed during the 12 month period between summer 2002 and summer 2003.

[1] One pin was found laying on the bank nearby.

The relative erosion amounts given in the table are, for the most part, fairly intuitive. For example, the erosion observed in the 'east channel,' and the 'left channel' (above the Kelsall boat launch) ranged from minimal to 10 cm. Note that boating traffic in the left channel is minimal. During the 2002 field study, the flow in the east channel was found to be on the order of 15 m^3 s^{-1}. During the 2003 field study, the flow in the left channel was measured with a wading survey and was found to be roughly 17 m^3 s^{-1}.

The erosion observed in the middle channel above the Kelsall landing was much greater, averaging 35 cm. The flow in this channel was measured in 2002 to be 73 m^3 s^{-1} and in 2003 to be 67 m^3 s^{-1}. There are numerous reasons for these relatively large erosion values. First of all, the greater river discharge is expected to result in greater erosion. Second of all, the wake heights recorded in these areas during the 2002 study were quite high, in the neighborhood of 25 cm. Third, the banks where these pins were installed were fairly 'raw,' lacking substantial woody vegetation. The fairly exposed nature of these banks also manifested itself in the turbidity measurements of 2002, which showed that significant sediment sloughed off due to wake impact.

Most interesting, perhaps, are the values for erosion observed in the channel leading to Sheep Canyon Lake. The discharge measurements from 2002 revealed the flow in that channel to be exceedingly low, on the order of 1 m^3 s^{-1}. This, given the channel geometry, corresponds to an area-averaged flow velocity of less than 10 cm s^{-1}. Such a low velocity suggests that erosion due to streamflow is negligible. While not definitive, this nevertheless points to boating activity as the agent causing erosion in this channel. Note that this portion of the route run by the tour operator is an 'out and back,' with the ramification that each boat travels the channel twice. The wake measurements from 2002 showed that the maximum wave heights were an extremely strong function of boat speed. Planing speeds near 20 mph were capable of generating wakes on the order of 30 cm. Extremely slow, 'no-wake' speeds, on the other hand, successfully reduced wake heights below 10 cm. It must be stressed that boat speed must be extremely slow (less than 5 mph) in order to take advantage of this reduction; one trial with the boat travelling at 6 mph resulted in wake heights of $\sim$25 cm.

3.1.1 Second Year Erosion Data

During the summer of 2004, ADFG personnel returned to a limited number of erosion pin sites to record additional values. As the pins *were not reset* during the 2003 field study, the values tabulated in Table 3.2 reflect cumulative erosion amounts for the 24 month period between summer 2002 and summer 2004. As the data indicate, continued erosion was observed at all sites.

Location	Notes	Upper Pin (cm)	Middle Pin (cm)	Lower Pin (cm)	Average (cm)
SHEEP CYN	West bank	59.7	35.6	12.7	36.0
	East bank	0	10.2	17.8	9.3
EAST CHAN	West bank	15.2	12.7	27.9	18.6
	East bank	0	2.5	8.9	3.8
MC3 WEST		44.5	49.5	36.8	43.6
EC2	Downstream location	7.6	11.4	20.3	13.1
KELSALL		2.5[2]	5.1	5.1	4.2

Table 3.2: Erosion pin data for the Upper Chilkat River. Values given reflect the amount of erosion observed during the 24 month period between summer 2002 and summer 2004.

[2] Recall that all three pins were missing during the 2003 survey. New pins were placed at that time and these values reflect the 12 month period between summer 2003 and summer 2004.

3.2 Near-Bank Hydraulics

The wading surveys of the 2002 field study give information on the average flow properties in the various channels studied, but yield little in terms of the details of the flow near the banks. One of the objectives of the 2003 field study was to take a closer look at the structure of the mean and fluctuating velocity fields in the near-bank regions. Of additional interest was the structure of the turbidity in the near-bank regions.

3.2.1 Velocity Data

To measure the velocity, use was made of a SonTek 10 MHz acoustic doppler velocimeter (ADV), shown in Fig. 3.6. The ADV is capable of measuring three components of velocity (u, v, w) at sampling rates of up to 20 hertz. Note that u denotes the component of velocity in the streamwise direction, v the component in the lateral direction and w the component in the vertical direction. The ADV operates by emitting acoustic energy from a transmitter located at the end of the probe. These signals are relected off of tiny particles in the water and scattered back to three receivers. By analyzing the Doppler shift in the frequency, the velocity of the particles, and, by assumption, the carrier water can be deduced.

Figure 3.6: Sontek ADV in 'side-looking' mode.

For the measurements described below, the ADV was used in its 'downward-looking' mode. The probe was mounted, as shown in Fig. 3.7, on a telescoping surveying tripod, equipped with levels. In this fashion, the probe could be placed at a prescribed horizontal and vertical location relative to the bank. Through a combination of vertical and horizontal traverses of the probe, a relatively detailed two-dimensional map of the velocity field can be built up.

Figure 3.7: Sontek ADV in 'downward-looking' mode.

A schematic configuration is shown in Fig. 3.8. As shown, a coordinate system is fixed at the waterline at the bank. In this case, the positive x axis is pointing upstream, the positive y axis is pointing across the river and the positive z axis is pointing upwards.

Disney Channel East Bank

Velocity surveys were performed at several locations, the first of which was along the east bank of the Disney Channel, slightly downstream of where it branches off from the main channel of the Chilkat River. The discharge in this channel could not be measured directly, but was estimated to be on the order of 50 $m^3\ s^{-1}$. The ADV was positioned at 23 different locations and, at each location, a long time-series of three-dimensional velocity was obtained. From each time series, and for each component, the mean velocity and the root-mean-square value of the fluctuating velocity was determined.

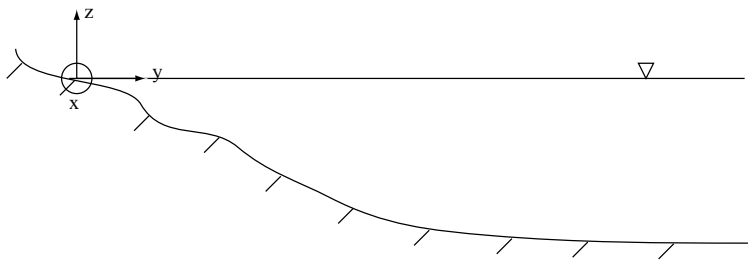

Figure 3.8: Schematic of near-bank bathymetry. Note that the positive x axis is pointing out of the page.

In addition, the Reynolds stresses were determined. These stresses are the time-averages of the products between two fluctuating velocities, e.g. $\overline{u'v'}$. Table 3.3 summarizes these data.

y (m)	z (cm)	$\overline{u}$ (cm s^{-1})	$\overline{v}$ (cm s^{-1})	$\overline{w}$ (cm s^{-1})	$\sqrt{\overline{u'^2}}$ (cm s^{-1})	$\sqrt{\overline{v'^2}}$ (cm s^{-1})	$\sqrt{\overline{w'^2}}$ (cm s^{-1})	$\overline{u'v'}$ (cm^2 s^{-2})	$\overline{u'w'}$ (cm^2 s^{-2})	$\overline{v'w'}$ (cm^2 s^{-2})	Turbidity (NTUs)
1.55	-13.2	-25.7	2.55	-2.35	3.23	3.20	1.88	-0.93	2.09	-0.85	
1.55	-25.1	-24.5	2.64	-3.29	4.14	2.84	2.21	-2.41	4.12	-0.26	141
1.55	-30.4	-24.6	3.22	-3.36	3.38	3.04	1.87	1.29	2.53	-0.56	137
2.44	-13	-32.8	6.17	-3.05	4.01	3.08	2.23	-1.90	2.09	-1.04	
2.44	-33	-30.3	2.24	-2.48	4.34	3.16	2.83	5.01	4.04	1.31	133
2.44	-53.1	-27.9	3.13	-0.14	3.81	3.22	2.61	-1.07	2.79	-1.15	134
2.44	-63.2	-22.7	4.35	1.01	3.54	3.23	1.95	-2.25	2.53	-2.61	134
3.58	-15.1	-52.1	2.73	-5.07	6.60	5.47	3.89	12.1	6.11	1.52	
3.58	-35.1	-48.9	4.28	-4.55	7.36	6.49	5.34	1.87	13.1	1.18	140
3.58	-55.1	-43.4	8.65	-3.50	6.84	5.83	5.70	1.23	16.5	0.68	148
3.58	-75.1	-33.0	8.72	-1.28	6.67	5.39	4.51	-7.84	9.63	-0.09	136
3.58	-90.6	-21.9	7.53	-0.37	5.61	4.79	2.23	-4.08	3.57	-1.15	133
4.67	-15.6	-58.9	0.63	-5.77	6.85	6.09	4.27	9.70	7.76	0.04	
4.67	-35.6	-60.6	1.79	-6.49	8.39	6.40	5.25	15.4	16.1	-1.87	141
4.67	-55.6	-49.2	8.07	-4.96	7.12	6.99	5.69	4.20	10.8	-12.1	133
4.67	-75.6	-46.5	4.43	-5.51	8.24	7.25	6.09	10.7	14.5	-12.3	131
4.67	-95.6	-35.6	-0.87	-3.66	6.72	6.06	4.95	8.67	12.1	-4.59	126
4.67	-100.8	-32.9	-2.55	-2.46	7.69	6.97	4.28	20.7	4.66	-7.04	123
6.17	-17.9	-67.6	9.45	-6.47	6.76	5.59	4.13	5.19	3.11	-0.98	
6.17	-37.9	-71.4	9.89	-6.25	7.07	5.70	4.69	5.67	2.83	-1.94	137

Table 3.3: Summary of velocity and turbidity data for the Disney Channel (east bank) site.

6.17	-57.9	-71.6	5.06	-4.50	7.84	6.36	5.35	5.06	11.7	-1.60	138
6.17	-77.9	-65.2	1.35	-2.50	8.04	6.32	5.41	13.9	14.2	-2.98	138
6.17	-97.9	-59.0	2.98	-0.54	9.08	6.48	4.03	12.0	9.37	-4.56	138

Table 3.3: (continued)

To give a graphical feel to some of this data, consider first the streamwise (in the x direction) velocity u. Figure 3.9(a) shows a two-dimensional contour map of $\overline{u}$, which is the time-averaged, or mean, value. Figure 3.9(b) shows a two-dimensional contour map of the turbulent kinetic energy, which is given by

$$k = \frac{1}{2}(\overline{u'^2} + \overline{v'^2} + \overline{w'^2}). \tag{3.1}$$

The structure of this mean flow is as expected, with boundary layer behavior being observed both in the vertical and the lateral directions.

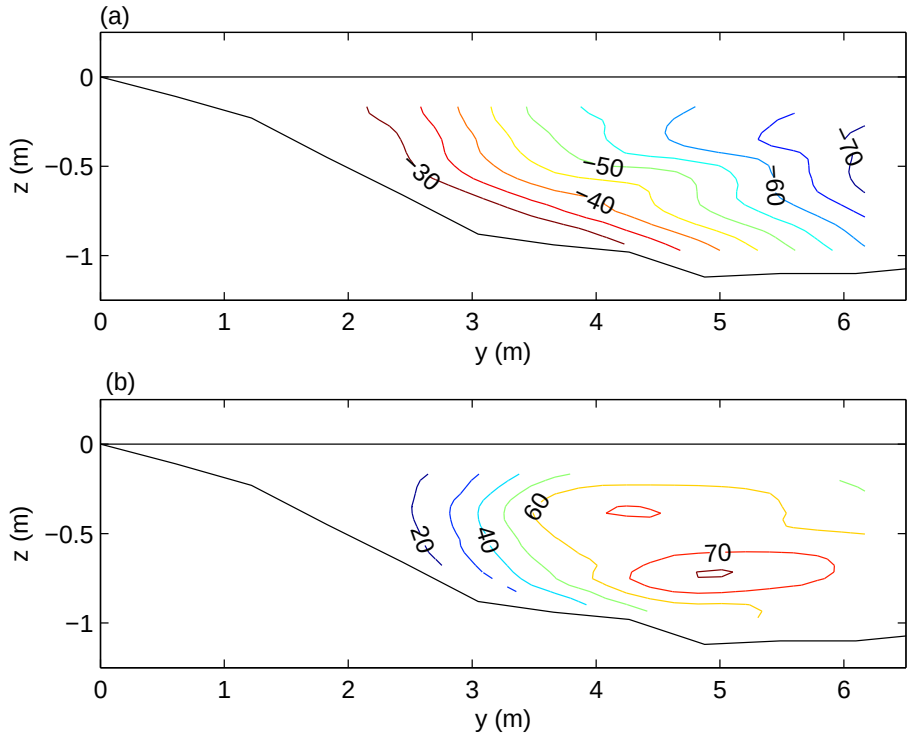

Figure 3.9: Near-bank velocity data from the Disney Channel east bank site. View is downstream. (a) - contours of mean streamwise velocity $\overline{u}$ in units of cm s^{-1}. (b) - contours of turbulent kinetic energy k in units of cm^2 s^{-2}.

The structure of the turbulent velocity is not as clearly evident, but merits some discussion. For simplicity, consider for the moment flow in a wide rectangular channel, so that the flow is essentially two-dimensional. In this

case, of course, the mean flow varies asymptotically from zero at the bed to a maximum at the free surface. Turbulent quantities, however, are found to exhibit the opposite behavior with larger values near the boundary than near the free surface. This is because the production of turbulence originates from the shear at the boundary.

Nezu and Nakagawa (1993) give the following empirical formulae for the vertical distributions of turbulent quantities in an open channel flow:

$$\frac{\sqrt{\overline{u'^2}}}{u_*} = 2.30e^{-z/h} \tag{3.2}$$

$$\frac{\sqrt{\overline{v'^2}}}{u_*} = 1.63e^{-z/h} \tag{3.3}$$

$$\frac{\sqrt{\overline{w'^2}}}{u_*} = 1.27e^{-z/h} \tag{3.4}$$

$$\frac{k}{u_*^2} = 4.78e^{-2y/h}. \tag{3.5}$$

Note that the origin of the z coordinate now lies on the bed, h is the flow depth, and u_* is the shear velocity. This shear velocity is related to the shear stress on the bed, τ_0, through the relationship $u_* = \sqrt{\tau_0/\rho}$, where ρ is the density of the water.

From these formulae, it can be shown that the depth-averaged value of $\sqrt{\overline{u'^2}}$ is approximately 150% of the shear velocity. From the data, this yields a shear velocity of about 4.2 cm s^{-1} for the present field site. Performing similar estimates based upon the data and formulae for the vertical and lateral turbulent velocities yields estimates of 5.0 and 5.2 cm s^{-1}. Thus, an overall average of 4.8 is adopted for the shear velocity.

If, on the other hand, the formula for the turbulent kinetic energy is considered, depth-averaging and use of the data suggests a shear velocity of 5.4 cm s^{-1}. The point is that all of the turbulent velocity data provide fairly consistent estimates.

Disney Channel West Bank

This site was directly across the channel from the previous site. As before, the two-dimensional structure of the velocity in the near-bank area was determined and the data are summarized in the table below. The contours of

mean streamwise velocity and turbulent kinetic energy are given in Fig. 3.10. Following the same reasoning as discussed above, estimates of shear velocity are obtained from the root-mean-square values of the fluctuating velocity components and from the turbulent kinetic energy. These varying estimates give, on average, a value of 4.8 cm s^{-1}, similar to that found for the east bank site.

y (m)	z (cm)	$\overline{u}$ (cm s^{-1})	$\overline{v}$ (cm s^{-1})	$\overline{w}$ (cm s^{-1})	$\sqrt{\overline{u'^2}}$ (cm s^{-1})	$\sqrt{\overline{v'^2}}$ (cm s^{-1})	$\sqrt{\overline{w'^2}}$ (cm s^{-1})	$\overline{u'v'}$ (cm^2 s^{-2})	$\overline{u'w'}$ (cm^2 s^{-2})	$\overline{v'w'}$ (cm^2 s^{-2})	Turbidity (NTUs)
0.76	-21.7	-1.12	0.92	0.80	2.20	1.91	1.29	-0.82	0.52	0.77	
0.76	-26.8	-0.08	1.34	0.03	2.98	2.81	1.37	-1.73	-0.44	0.82	
1.52	-17.0	-14.5	0.89	-1.88	5.70	3.69	2.61	-11.1	-0.07	-0.40	
1.52	-32.0										105
1.52	-47.0	-8.08	-3.00	-4.49	4.76	4.03	2.94	-5.64	3.86	2.26	95
1.52	-62.0	-1.65	-3.87	-4.85	3.34	2.71	2.23	-2.60	1.22	0.93	91
2.51	-9.6	-41.8	15.7	-3.69	6.71	5.81	3.95	-11.8	-7.19	0.24	
2.51	-29.6	-46.7	18.4	-4.35	6.14	5.79	4.43	-10.2	-3.53	-0.38	111
2.51	-49.6	-45.6	17.9	-4.44	8.36	7.81	6.44	-30.4	18.4	-10.2	111
2.51	-69.6	-34.0	11.7	-3.65	8.60	8.47	6.50	-29.3	18.4	-10.2	105
2.51	-89.6	-23.5	8.77	-5.05	7.44	8.17	5.10	-15.6	16.8	-0.54	96
3.40	-16.2	-56.5	24.5	-8.07	6.10	6.54	4.40	-12.3	-1.90	-2.56	
3.40	-36.2	-63.5	27.9	-8.39	6.25	5.74	4.63	-7.67	1.88	-2.49	117
3.40	-56.2	-69.3	7.01	-7.68	6.78	5.56	5.04	-3.38	6.51	0.66	115
3.40	-76.2	-65.7	5.57	-6.35	8.72	6.85	5.97	-5.10	20.3	2.39	125
3.40	-96.2	-50.4	13.8	-5.10	10.4	9.00	7.20	21.5	38.1	-2.30	135
3.40	-111.3	-34.8	11.8	-4.25	14.7	11.3	5.94	-46.1	36.1	-6.87	119

Table 3.4: Summary of velocity and turbidity data for the Disney Channel (west bank) site.

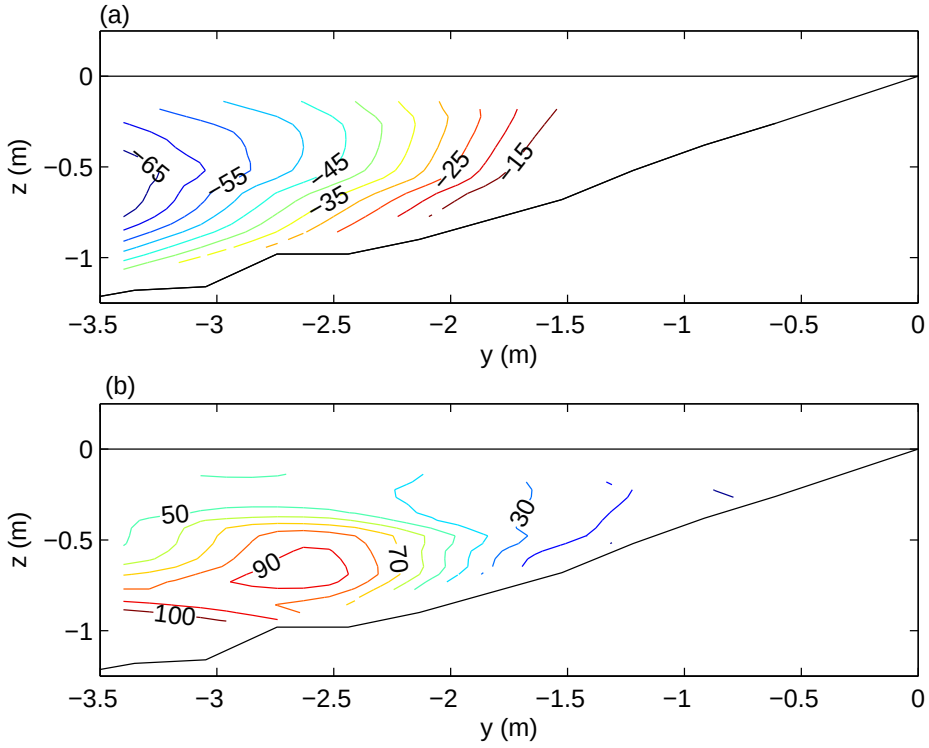

Figure 3.10: Near-bank velocity data from the Disney Channel west bank site. View is downstream. (a) - contours of mean streamwise velocity $\overline{u}$ in units of cm s^{-1}. (b) - contours of turbulent kinetic energy k in units of cm^2 s^{-2}.

Dry Lake

This site, which was one of the sites studied during the 2002 field project, lies on the west bank of the southern end of Dry Lake. The river here carries a flow that is approximately 50% greater than that in the Disney Channel. The obtained velocity data are presented in the Table below and are shown graphically in Fig. 3.11. If the data are considered along with the empirical formulae of Nezu and Nakagawa (1993), an average shear velocity of approximately 7.5 cm s^{-1} is found. This higher value is intuitive, given that the discharge, and hence shear stress, is greater at this site.

y (m)	z (cm)	$\overline{u}$ (cm s^{-1})	$\overline{v}$ (cm s^{-1})	$\overline{w}$ (cm s^{-1})	$\sqrt{\overline{u'^2}}$ (cm s^{-1})	$\sqrt{\overline{v'^2}}$ (cm s^{-1})	$\sqrt{\overline{w'^2}}$ (cm s^{-1})	$\overline{u'v'}$ (cm^2 s^{-2})	$\overline{u'w'}$ (cm^2 s^{-2})	$\overline{v'w'}$ (cm^2 s^{-2})
0.36	-10.0	-5.41	-9.81	0.43	7.23	5.69	5.77	-11.3	-2.81	-2.09
0.36	-20.0	-6.34	0.63	2.45	7.29	5.88	6.35	-14.9	3.29	4.43
0.36	-30.0	-8.83	3.51	1.47	7.12	5.68	6.10	-14.9	-1.63	2.73
0.36	-35.0	-9.36	5.30	1.80	8.65	5.91	5.85	-16.5	-1.55	10.6
0.94	-10.0	-49.1	1.11	-2.75	11.0	7.74	6.04	-26.2	-10.2	-2.65
0.94	-25.0	-57.5	4.86	-3.36	8.48	7.28	6.70	-15.5	1.79	-3.90
0.94	-40.0	-55.4	4.54	-3.54	9.42	7.40	6.31	- 18.93	11.7	0.89
0.94	-55.0	-44.8	-5.64	-2.09	12.1	8.32	7.13	-14.2	21.2	11.5
0.94	-70.0	-28.9	-6.29	-1.58	11.1	8.71	6.08	-16.1	14.7	12.2
1.65	-10.0	-76.4	1.51	-8.06	9.48	7.89	5.12	-16.8	15.4	0.21
1.65	-25.0	-75.0	1.30	-8.81	10.8	8.59	6.97	-6.4	28.1	4.11
1.65	-40.0	-65.8	0.24	-5.60	11.4	8.72	7.51	-0.86	35.9	0.11
1.65	-55.0	-59.6	-4.86	-5.72	11.7	8.43	7.01	8.53	38.7	-0.48
1.65	-70.0	-47.8	-7.81	-4.23	12.1	9.59	7.44	6.08	43.4	3.34
1.65	-80.0	-36.8	-9.20	-3.60	10.8	10.2	6.05	8.33	26.5	4.85

Table 3.5: Summary of velocity data for the Dry Lake site.

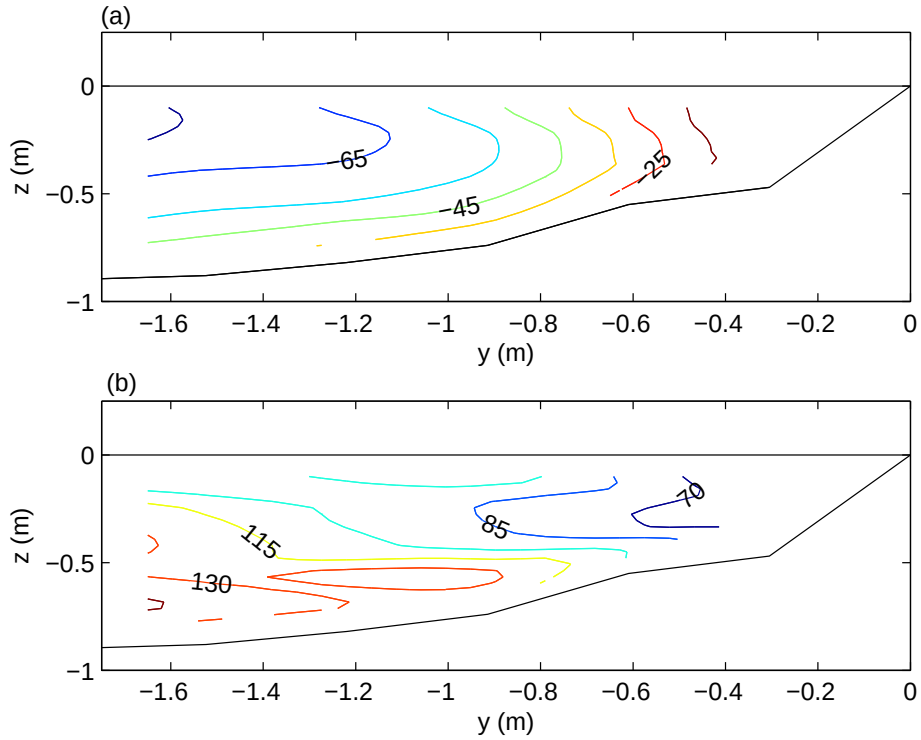

Figure 3.11: Near-bank velocity data from the Dry Lake site. View is downstream. (a) - contours of mean streamwise velocity $\overline{u}$ in units of cm s^{-1}. (b) - contours of turbulent kinetic energy k in units of cm^2 s^{-2}.

3.2.2 Turbidity Data

The report from the 2002 field project extensively documented the increases in near-bank turbidity that would occur in response to wakes of differing sizes. Elevated turbidities of two to five times the ambient value were commonly observed, with occasional amplifications of up to 10. During the 2003 field project, a more extensive survey of the background turbidity in the river was undertaken.

First, an OBS sensor was mounted in tandem with the ADV during the velocity trials described above. In this fashion, just as the two-dimensional structure of the velocity could be evaluated, so could the structure of the turbidity. The observed turbidity values are given in the tables of the previous

section and indicate that there is little spatial variability. A typical value of ambient turbidity is $\sim$ 100 NTUs.

In addition to these measurements, representative values of ambient turbidity were obtained in a second manner. At a total of seven sites, ranging from Wells Bridge in the south to the Kelsall Confluence in the north, 'transects' of turbidity were obtained. These were obtained by idling across the width of the river over a 2 minute period at each site. During the traverse, turbidity data were continuously being taken at a depth of $\sim$ 50 cm below the surface. Upon completion of the traverse, the data were averaged, in order to arrive at a representative value. As Table 3.6 indicates, there was, again, little variability in the data, with all sites pointing to approximately 100 NTUs.

Location	Average Turbidity (NTUs)
Main channel, just above Disney Channel	118
Disney Channel	93
East Channel	115
Main Channel, above Kelsall Landing	105
Kelsall confluence	91
Wells Bridge	120

Table 3.6: Turbidity data, as obtained from channel 'transects.'

3.2.3 Near-Bank Dye Study

The level of the turbulence in an open channel flow can also be estimated by assessing the flow's ability to mix a scalar. In laminar flows, a scalar such as a passive dye will mix only by the relatively slow process of molecular diffusion. In a turbulent flow, the dye is more efficiently mixed by turbulent eddies of varying length and time scales. For a thorough introduction to the mechanics of river mixing, the reader is referred to Rutherford (1994).

In the interest of a brief introduction, consider the schematic overhead view of a river of rectangular cross section and large aspect ratio (i.e. width $\gg$ depth) shown in Fig. 3.12. Next, consider the situation where dye, of some known initial concentration, is steadily discharged at the bank at $x = 0$. As the flow carries the dye downstream, turbulent eddies will very rapidly mix the dye uniformly across the depth of the flow. At this point, the dye

concentration field becomes two-dimensional, exhibiting variation only in the $x - y$ plane. With further downstream distance, the turbulent eddies will continue to mix the dye across the width of the river. As a consequence, the concentrations observed at the bank will decrease with increasing x.

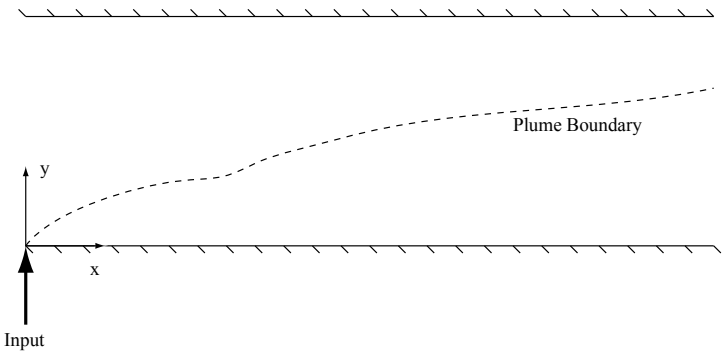

Figure 3.12: Top-view schematic of a steady-input, bank-discharge dye study. Note the widening of the dye plume with downstream distance.

Experimental Instrumentation

For the present experiment, measurements of dye concentration were made with a Turner 10-AU Field Fluorometer. The Turner Fluorometer has a sensitivity of 10 parts per trillion of Rhodamine WT (which was the dye used). The fluorometer was used in continuous sampling mode, which means that a small centrifugal pump was used to continuously pump river water through the flow-cell of the fluorometer. An internal data logger was used to record the time-series of fluorescence. Subsequent to the field measurements, the data were downloaded to a laptop for analysis.

Experimental Procedure

A steady-input bank-discharge dye study was conducted on the west bank of Dry Lake. This site was chosen as velocity data had previously been obtained at the site. This would allow for a comparison / verification of the results obtained by the two methods.

The experiment was conducted by first preparing a dilute solution of Rhodamine WT dye. Rhodamine WT dye is commonly sold in solution with

20% active ingredient. As this solution is somewhat more dense than water, it is common to further dilute the solution with ambient water. For the present experiment, a solution was prepared that had a concentration of 5.1%, by volume, of the initial 20% solution.

This solution was then discharged, at a rate of 48 ml min^{-1} at the bank of the river. After allowing some time for the dye plume to establish itself, measurements were made at a variety of x and y locations downstream of the injection point. At each location, data were sampled continuously at a rate of 1 Hz for approximately 2 minutes. Each time-series was then averaged to obtain an average value of concentration at that point. The data, in units of ppb (parts per billion) are summarized in Table 3.7.

A two-dimensional contour plot of the concentration field is shown in Fig. 3.13. It clearly shows the expected behavior, which is Gaussian. With increasing downstream distance, the concentration at the bank decreases. At the same time the plume steadily widens. Another way of looking at the data is to superimpose lateral profiles of concentration at the different x locations. This is shown in Fig. 3.14. Again, the features of the centerline decrease in concentration and the widening of the dye plume are readily evident.

In order to extract useful information from these data, use is made of the theoretical equation for transverse mixing, given by

$$C(x,y) = \frac{\dot{m}}{h\sqrt{4\pi K_y x V}} \exp\left(\frac{-Vy^2}{4K_y x}\right). \tag{3.6}$$

In this equation, $\dot{m}$ is the mass flow rate of the dye injection, K_y is the transverse dispersion coefficient, and h is the water depth. To make use of this equation, care must be taken to put all quantities into consistent units. For example, the recorded concentrations must be converted from ppb to kg m^{-3}.

The data can be fit to this equation, in a least-squares sense, treating both the flow velocity and the dispersion coefficient as unknown parameters. These parameters are repeatedly adjusted until the best fit is obtained. Upon doing so, a dispersion coefficient of 0.016 m^2 s^{-1} and a velocity of 0.38 m s^{-1} are obtained. Referring to Fig. 3.11, it is seen that this velocity is indeed a reasonable representative value for the average near-bank velocity observed near the Dry Lake site. If the obtained parameters are then used to calculate the theoretical concentration field (Fig. 3.15), it is seen that the results agree quite nicely with the field data (Fig. 3.13).

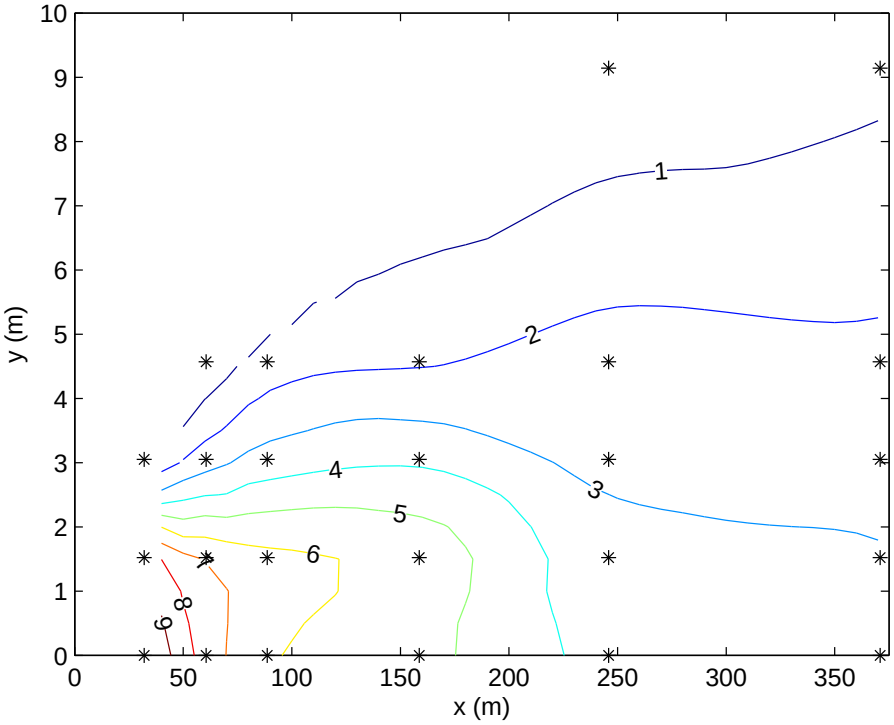

Figure 3.13: Contours (in ppb) of dye concentration for the Dry Lake near-bank steady-discharge dye study. The symbols denote the locations where the dye concentration was measured.

Further confirmation of the general validity of the obtained dispersion coefficient can be found in Rutherford (1994). In Chapter 3 of his text, he suggests that the transverse dispersion coefficient for gently irregular channels falls in the range of 30 to 90% of the product of water depth and shear velocity. For the Dry Lake site, this yields a range of shear velocity from 4 to 10 cm s^{-1}, which is very much in line with the velocity results previously discussed.

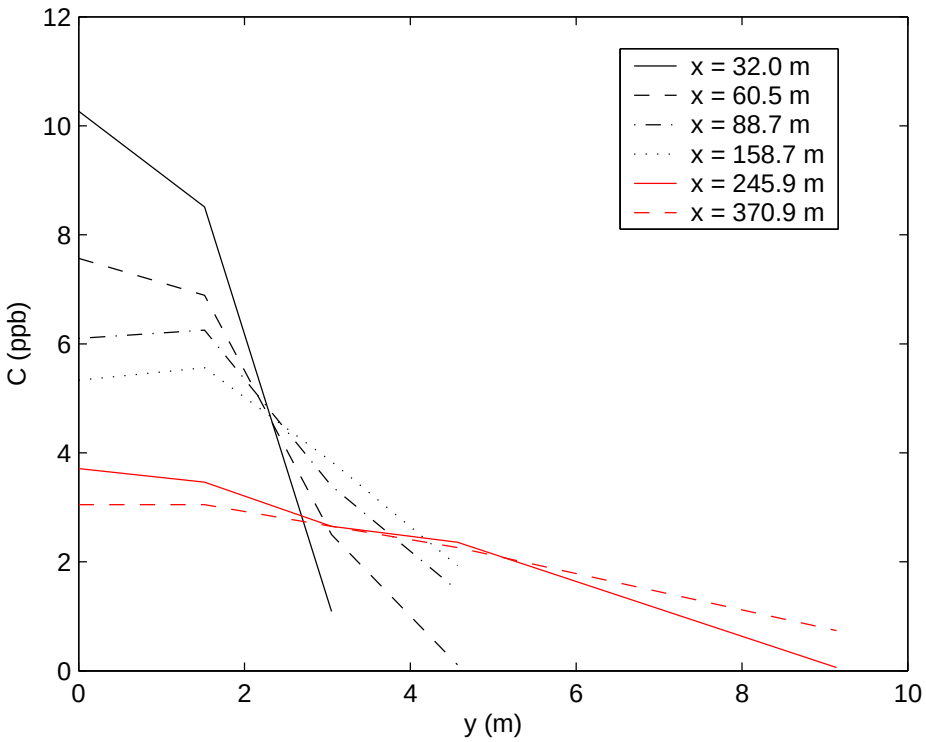

Figure 3.14: Lateral profiles of dye concentration at various x locations.

x (m)	y (m)	C (ppb)
32	0	10.27
32	1.52	8.51
32	3.05	1.09
60.5	0	7.57
60.5	1.52	6.89
60.5	3.05	2.50
60.5	4.57	0.11
88.7	0	6.10
88.7	1.52	6.25
88.7	3.05	3.39
88.7	4.57	1.48
158.7	0	5.33
158.7	1.52	5.56
158.7	3.05	3.84
158.7	4.57	1.93
245.9	0	3.71
245.9	1.52	3.46
245.9	3.05	2.65
245.9	4.57	2.36
245.9	9.14	0.06
370.9	0	3.05
370.9	1.52	3.05
370.9	3.05	2.65
370.9	4.57	2.26
370.9	9.14	0.74

Table 3.7: Rhodamine dye concentrations observed during steady-input, bank-discharge dye study at Dry Lake.

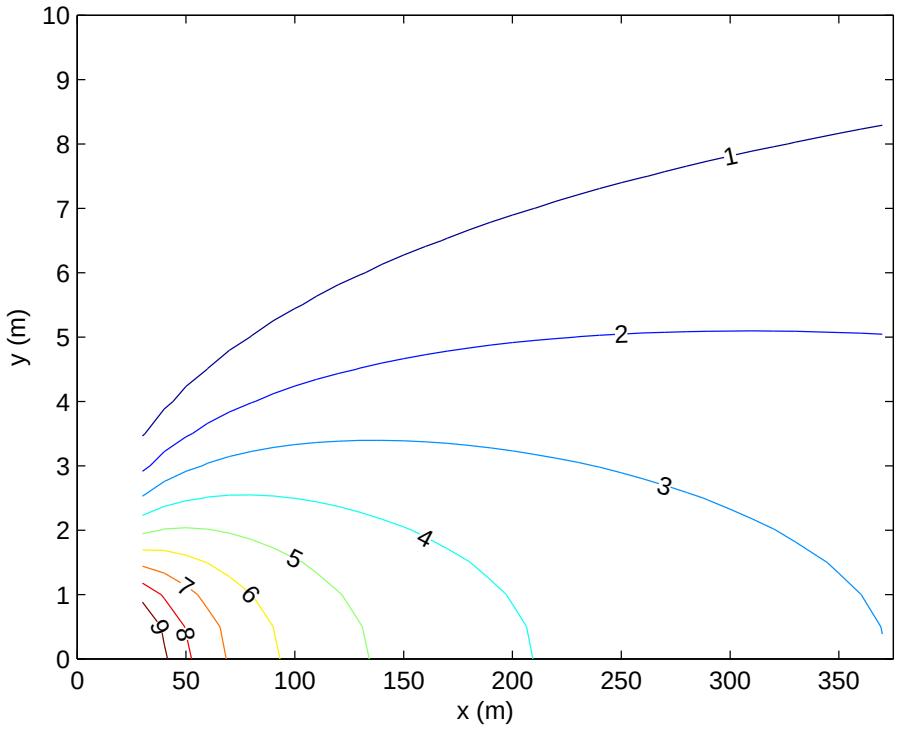

Figure 3.15: Theoretical predictions for dye concentration at the Dry Lake site, using the best-fit values for flow velocity and dispersion coefficient.

Chapter 4

Laboratory Study

Upon returning from the field, the goal of the laboratory study was to determine whether or not elevated levels (above ambient) of turbulence and turbidity have a measurable biological impact on rearing coho salmon. If so, then some level of regulation of boating traffic, during sensitive times of the year, would be justified.

In reducing this to an idealized laboratory study, some compromises had to be made. These compromises reflect the competing needs of the reproduction of the field environment and the practical and economic considerations of the laboratory environment. In the end, two different experimental trials were devised, so as to isolate the separate effects of fluid turbulence and suspended sediment loading. In the first trial, coho salmon fry were exposed to repeated, brief episodes of turbulent flow. The repetition and relatively brief loading were intended to roughly reproduce the fact that, in the field, sets of breaking waves impact the river banks intermittently throughout the day. In the second trial, coho salmon fry were exposed to similarly repeated and brief episodes of high turbidity, intended to reproduce the field observations of sediment sloughing off of the banks.

4.1 Experimental Facilities

In order to discern a measurable trend, if any, in impact, it was decided that a minimum of three treatments (turbulence / turbidity levels) were needed. For statistical reasons, it was further decided that the experiments should be conducted in triplicate. The three treatments, plus a control, therefore

required a total of 12 experimental tanks.

These tanks were each nominally 91 cm in length, 45 cm in width, and filled with water to a depth of 38 cm. The general idea of the arrangement of the tanks is shown in Fig. 4.1. The tanks were encased in 1.25 cm thick blueboard insulation and had lids to further insulate the tanks and to secure jumping salmon. The 12 tanks were on a common sterilization and filtration loop. The biofilter media, having a high surface area, are colonized by bacterium that metabolizes nitrogenous wastes. The sterilization comes from ultraviolet light.

4.1.1 Turbulence Trial

Creating a spatially uniform level of turbulence in a flow is a rather difficult task. Even in the simple case of two-dimensional open channel flow over a flat bottom, the distributions of mean flow and turbulent quantities are variable. Regarding the turbulent quantities, this is due to the fact that the source of production of the turbulent kinetic energy is the shear at the boundary. Thus, the layers of fluid closer to the boundary experience a higher level of turbulence than those farther away.

One well-documented way of generating turbulence in a closed fluid domain is through the oscillation of a 'grid' of rods. In this case, the turbulence characteristics of the flow will be functions of the rod diameter, the spacing between the rods, and the stroke and frequency of the grid motion.

Another well-documented flow where the turbulence characteristics are well known is a 'jet flow.' In this situation, a high-velocity jet of water discharges from a round orifice into an ambient receiving water body. As shown, in idealized form in Fig. 4.2, there is an initial 'zone of establishment,' followed by a 'zone of established flow.' Both zones have been very well studied in the past, with the consequence that the spatial variation of the turbulence characteristics, as functions of the jet velocity and diameter, are known.

Motivated by this, it was decided to set the turbulence levels in the tanks by using, in each tank, an array of four nozzles. As shown in Fig. 4.3, an intake was positioned at the far right end of the tank. The intake was fitted with a screened inlet, in order to prevent the entrainment of fish into the system plumbing. Water then passed through, in turn, a 1 horsepower centrifugal pump, a valve, and a flow meter. After passing through the flow meter, the plumbing returned to the far left end of the tank, where it

branched into four lines. The four lines each terminated in a 1 cm diameter nozzle that was mounted flush into a 'false wall.'

The result of this configuration is a set of four overlapping jet flows. Both the mean and turbulent velocities are highest close to the jet origins. With both increasing streamwise distance (i.e. along the jet axis, away from the jet origin) and lateral distance (i.e. perpendicularly away from the jet axis) these quantities decrease. For the purposes of these experiments, the spatial variability in the turbulent flow field was removed by considering a volume-averaged value. While, in principle, it is possible for an individual fish to 'hide' in a low-turbulence region of the tank, informal observations suggested that this did not happen. Instead, the jet flows were strong enough to repeatedly entrain the fish into the high-turbulence region of the tank.

4.1.2 Turbidity Trial

For the turbidity trial, which followed the turbulence trial, it was found that some modification to the tanks was required. The key issue here was the ability of the apparatus to keep in complete suspension the sediment in the tank. Given the slightly cohesive nature of the sediment used to set the turbidity levels, it was found that the the horizontal jets were incapable of doing so.

In their place, a single 2.5 cm diameter pipe was oriented vertically such that it terminated at the bottom of the center of the tank. The pipe was then capped off and eight evenly-spaced holes were then drilled around the circumference of the cap. This configuration resulted in eight jets, much like the spokes of a wheel, parallel to and just above the tank bottom. In addition, a ninth hole, pointing downwards, was drilled in the end of the cap. Initial trials revealed that this configuration was far superior to the horizontal jets in terms of fully scouring the tank bottom each time the pumps were turned on.

4.2 Experimental Procedures

4.2.1 General Details

The general experimental procedures were similar for the two sets of trials. In each case, the length of the trial was three weeks. To reproduce an episodic

loading environment, electronic timers were used to cycle the pumps on and off. The pattern was such that a pump would come 'on' for 5 minutes and then shut 'off' for 25 minutes. This pattern was repeated 8 times per day.

Fish were obtained from a hatchery in New York. The feed that was used during the experiment was similar to the feed used at the hatchery and was a sinking feed. A total of 50 fish were placed in each tank at the start of each trial. In order to assess impact, growth rate was adopted as the measure. To facilitate this, the fish were batch weighed at the beginning of each experiment (Fig. 4.4). Baking soda was used to anesthetize the fish for weighing. The concentration was adjusted to the amount of water in the tray in order to achieve rapid immobilization.

Throughout the course of the three week trial, mortalities, which were very few in number, were removed on a daily basis. At the conclusion of the three week trial, the fish were again batch weighed. Based upon these weights and the number of fish, a per-fish weight both before and after the trial could be determined. A comparison of the before and after average weight would then indicate the average growth rate of the fish in an individual tank.

4.2.2 Turbulence Trials

In the turbulence trials, there were three control (C) tanks, three low treatment (L) tanks, three medium treatment (M) tanks, and three high treatment (H) tanks. A summary of the circulation loop flow rates and jet source velocities for the three treatment levels is given in Table 4.1. Also given in the table is an estimate of the rate of energy dissipation in the tank. This is determined from the fact that a sharp inlet into a tank has a loss coefficient of $K_L = 1$. From this, the head loss is determined from $h_L = K_L V_0^2/(2g)$. Finally, the power, or rate of energy loss is given by $P = \gamma h_L Q$. In the table, the power is normalized by the mass of water, yielding units of Watts per kg.

Treatment Level	Q (liters sec^{-1})	V_0 (m s^{-1})	P/m (W kg^{-1})
L	0.95	3.01	0.028
M	1.6	5.03	0.13
H	2.2	7.00	0.35

Table 4.1: Circulation loop volumetric flow rates, jet source velocities, and energy dissipation levels for the three treatment levels in the turbulence trials.

To compare these dissipation values with the streamflow, recall that the estimates in Chapter 3 indicated shear velocities on the order of 5-8 cm s^{-1}. Based upon the formal definition of dissipation, in units of W kg^{-1}

$$\Phi = \frac{\partial \overline{V}}{\partial y}\left(\mu \frac{\partial \overline{V}}{\partial y} - \rho \overline{u'v'}\right), \tag{4.1}$$

and turbulent boundary layer solutions for open channel flow, one can show that the cross-sectionally averaged dissipation is

$$\Phi_{\text{avg}} = \frac{u_*^2 \overline{V}_m}{h}. \tag{4.2}$$

In the above equations, μ is the absolute viscosity of water and $\overline{V}_m$ denotes the depth averaged value of the mean velocity.

The present data therefore yield values of dissipation around $0.002-0.005$ W kg^{-1}. It must be noted, however, that these values underestimate the rate of dissipation in the vicinity of the banks and river bed. From (4.1), it is clear that dissipation is greater near the boundaries, where the velocity gradients are greatest. It can be shown that the 10% of the cross sectional area adjacent to the boundary contains about 80% of the dissipation. Thus, with this factor of 8 increase, it is reasonable to adopt the range of $0.016-0.04$ W kg^{-1} as being a 'baseline' value for the dissipation in the near-bank area due to streamflow. Thus, the low treatment level is seen to be comparable to the streamflow and the other treatments represent elevated levels.

4.2.3 Turbidity Trials

In the turbidity trial, as was previously stated, some modifications needed to be made in order to keep the sediment wholly in suspension while the pumps were turned on. In order to isolate the effects of the turbidity from the turbulence in this trial, the recirculating flows in all three treatment tanks were set to the same level. To further isolate the turbidity effects, the control tanks were equipped with plumbing and pumps identical to the treatment tanks. Put another way, the turbulence levels in *all* tanks were equal, ensuring that any observed systematic differences in growth rates among the tanks would be attributable to variations in turbidity levels. Given the need for pumps in the control tanks, along with the constraint on the number of pumps available, it was only possible to conduct this trial in duplicate, rather that in triplicate, as was done in the turbulence trial.

Treatment Level	Turbidity (NTU)
L	75
M	150
H	250

Table 4.2: Target turbidity levels for the three treatments.

The target turbidity levels for the three treatments (L,M,H) are given in Table 4.2. These levels were set using sediment brought back from the Chilkat River following the 2003 field experiment. Levels were measured using the OBS described in Chapter 3. As with the turbulence trial, the pumps operated in an intermittent fashion. During the 'on' periods, the sediment was completely suspended from the tank bottom and evenly distributed by the agitation in the tank. During the 'off' periods, the sediment would slowly settle out, such that the turbidity in the tank resembled an exponential-type decay. Over a period of about 15 minutes, the water would return to a fairly clear state.

Due to the master circulation loop that circulates water from all tanks through sterilization and filtration elements, the prospect of 'losing' sediment from the treatment tanks arose. Initial efforts to prevent this loss explored the possibility of shutting down the main loop during the portion of the day that the pumps were operational. This ultimately proved unsatisfactory from a water quality point of view.

As a result, some sediment loss was inevitable and was mitigated by adding additional sediment every two days. The amount of sediment lost during a single 'on' pump cycle is easily estimated through consideration of the conservation of mass equation. Given that the inflow returning from the filtration is sediment free, the equation for the concentration in a tank is given by

$$V\frac{dC}{dt} = -QC,$$

where V is the tank volume and Q is the through-flow. Solving this yields

$$C(t) = C_0 e^{-\frac{Q}{V}t},$$

where C_0 is some initial concentration. Given a tank volume of 150 liters and a flowrate of two liters per minute, it is found that, during a single five

minute ‘on’ cycle, approximately 7% of the sediment flows out of the tank and is trapped by the filtration system. The replacement of sediment every two days helped to keep the sediment levels at their target values.

Figure 4.1: Photograph of the experimental arrangement of tanks.

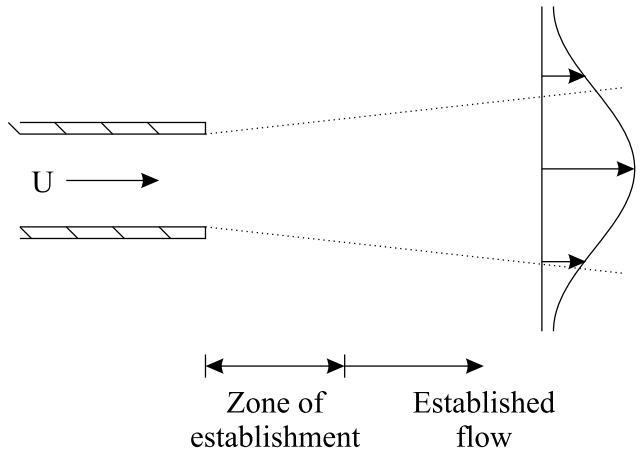

Figure 4.2: Schematic sketch of an axisymmetric fluid jet.

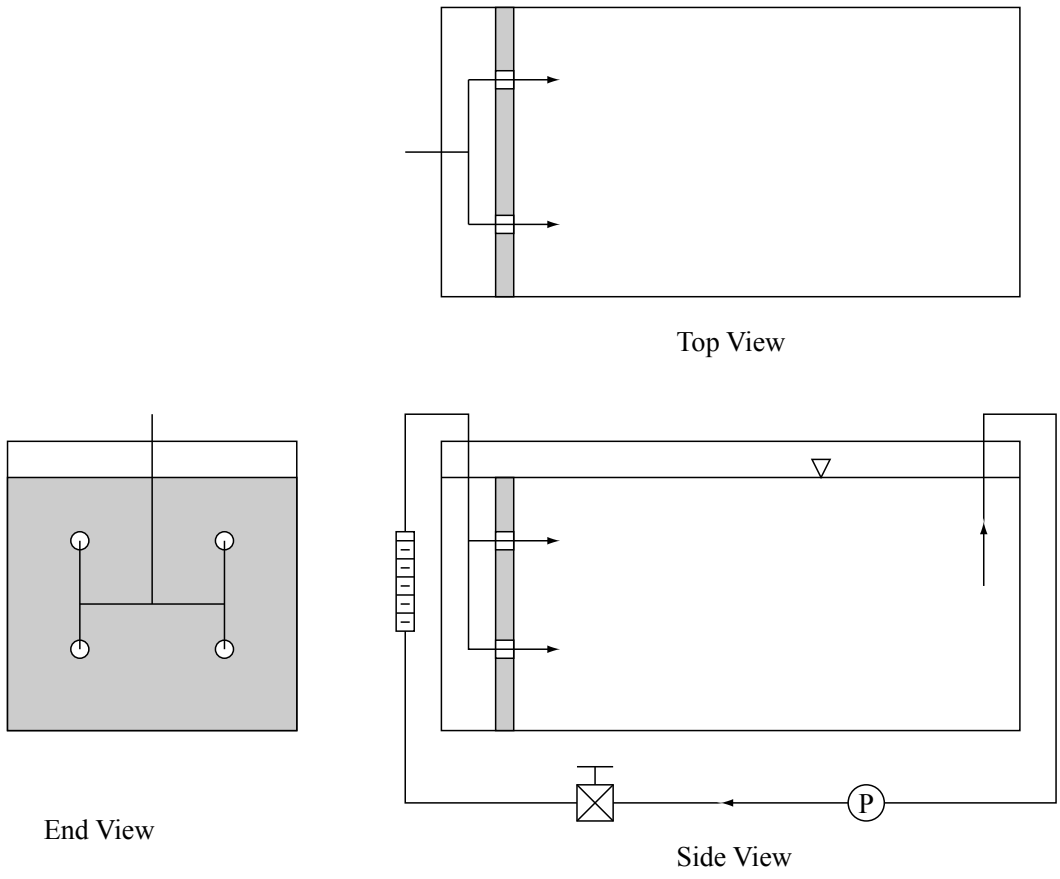

Figure 4.3: Schematic close-up views of the experimental apparatus for the turbulence trials.

Figure 4.4: Typical photograph of (sedated) fish being batch weighed.

4.3 Experimental Results

4.3.1 Turbulence Trials

The data from the turbulence trial is summarized in Table 4.3. The data are given in terms of total batch weight, sample size, and normalized weight. These data are provided for both the start and the finish of the trial. In addition, the average weight gain over the three week trial is provided. Finally, the ensemble averaged value (across the triplicate tanks) is provided.

	C1	C2	C3	L1	L2	L3	M1	M2	M3	H1	H2	H3
Start Data												
Total Weight (g)	86.48	88.28	88.74	98.4	105.7	93.98	95.40	98.12	92.90	86.94	91.92	93.38
Sample Size	50	50	50	50	54	48	50	50	50	50	50	50
Average Weight (g)	1.73	1.77	1.77	1.97	1.96	1.96	1.91	1.96	1.86	1.74	1.84	1.87
End Data												
Total Weight (g)	91.60	92.39	94.63	97.3	113.52	89.96	96.69	93.45	94.38	79.28	94.39	96.20
Sample Size	50	46	50	49	54	45	50	46	48	44	50	49
Average Weight (g)	1.83	2.01	1.89	1.99	2.10	2.00	1.93	203	1.97	1.80	1.89	1.96
Average Gain (g)	0.1024	0.2429	0.1179	0.0177	0.1448	0.0411	0.0257	0.0691	0.1083	0.0630	0.0494	0.0957
Ensemble Average Gain (g)		0.1544			0.0679			0.0677			0.0694	

Table 4.3: Summary of weight data for the turbulence trial.

4.3.2 Turbidity Trials

The data from the turbidity trial is summarized in Table 4.4. The data are given in terms of total batch weight, sample size, and normalized weight. These data are provided for both the start and the finish of the trial. In addition, the average weight gain over the three week trial is provided. Finally, the ensemble averaged value (across the duplicate tanks) is provided.

	C1	C2	L1	L2	M1	M2	H1	H2
Start Data								
Total Weight (g)	324.9	299.8	269.8	299.6	286.9	290	249.5	252.1
Sample Size	50	48	52	50	50	50	50	50
Average Weight (g)	6.50	6.25	5.19	5.99	5.74	5.80	4.99	5.04
End Data								
Total Weight (g)	355.1	357.8	336.9	351.3	340.5	354.7	305.1	300.1
Sample Size	50	48	52	50	50	50	50	50
Average Weight (g)	7.10	7.45	6.48	7.03	6.81	7.09	6.10	6.00
Average Gain (g)	0.60	1.21	1.29	1.03	1.07	1.29	1.11	0.96
Ensemble Average Gain (g)	0.91		1.16		1.18		1.04	

Table 4.4: Summary of weight data for the turbidity trial.

Chapter 5

Discussion and Conclusions

A near-bank hydraulic study of several sites on the Chilkat River was conducted during the summer of 2003. Measurements of mean velocity, turbulent velocity, and turbidity were made with an acoustic doppler velocimeter and an optical backscatter sensor. The goal of these measurements was to establish a 'baseline' of the typical hydraulic climate associated with the ambient flow of the river.

Subsequent to the field study, a laboratory study was conducted in order to determine the biological response of coho salmon fry to elevated levels of turbulence and turbidity. To assess impact, growth rate was adopted as a measure. Separate three week trials were conducted in order to assess the impacts of turbulence and turbidity.

5.1 Conclusions

Some of the key findings of this study include:

- Ongoing erosion pin measurements in the Chilkat River (since summer 2002) demonstrate steady erosion of the banks in response the the loadings on the banks. These loadings include the stream flow and the impacts of boat wakes. For the most part, larger erosion values are found in larger channels, but there are some exceptions to this generalization.

- Numerous estimation methods applied to the field data arrived at a shear velocity of $5 - 10$ cm s^{-1} in the vicinity of the banks. This

parameter is of broad use in terms of characterizing the mean and turbulent flow fields.

- Field measurements consistently placed the ambient, or background, turbidity of the river at $\sim$ 100 NTUs (nephelometric turbidity units).
- Laboratory trials revealed that the presence of fluid turbulence reduced the growth rate of salmon fry when compared to a control group exposed to no turbulence. However, the reduction in growth rate appeared not to be a function of the turbulence level in the tank.
- Laboratory trials revealed that the presence of turbidity did not seem to affect the growth rate of salmon fry. Moreover, the growth rate did not appear to be function of the turbidity level in the tank.

5.2 Discussion

Overall, the results suggest, within the parameters of the laboratory study, that coho fry are relatively unaffected physically by elevated levels of turbidity. Recall that these parameters include a three-week duration, episodic (eight five-minute exposures per day) loading, and approximately five-month old fry. Note as well that the 'high' treatment level corresponded to a turbidity 2.5 times that of the ambient streamflow. The relative lack of observed impact conflicts somewhat with the experiments discussed in Chapter 2.2, which demonstrated physical impacts at turbidity values lower than this level. In addition, some of the previous studies documented behavioral impacts. The present study was not able to make these types of behavioral observations.

The present results also suggest that, within the parameters of the laboratory study, that coho fry may be somewhat affected physically by *the presence* of elevated levels of turbulence. These parameters are equal to those described above, with the exception that the turbulence trial was conducted with approximately three-month old fry. This conclusion is reached by noting that all three turbulence treatment levels yielded a growth rate noticeably lower than the control group. The lack of variation in growth rate between the low, medium, and hight treatment levels, however, somewhat paradoxically suggests that the impact is independent of the actual *magnitude* of turbulence.

5.3 Recommendations

As discussed previously, the present study represents a compromise. The design of a laboratory study with any level of experimental control over the parameters inherently filters out the large degree of complexity and variability observed in the field. The main objective of the present study was to investigate, in a systematic way, the effects of periodic loading at levels above those of the ambient streamflow.

The reality on the Chilkat River is that salmon fry are mobile, not captive. As a result, the exact length and frequency of their exposure to loading from boat wakes are highly speculative. ADFG biologists have documented their general use of near-bank areas as habitat, but it is difficult to estimate the exact length of time that a specific fish spends in one location. Put another way, the mobility of fry acts as a mitigating factor. On the other hand, the recreational season on the river exceeds three months, whereas the experimental trial was only three weeks. This potentially longer exposure period may offset some of the mitigation described above.

Given the lack of experimental observations of severe physical impact, it seems reasonable to conclude that, at least in larger channels, low-level operation of boats poses minimal physical impact to salmon fry. The present study is unable to assess whether or not use levels on the Chilkat River pose any behavioral impact. In extremely small channels, such as that leading into Sheep Canyon Lake, where the hydraulic loading is similarly small, somewhat more caution may be warranted. As the erosion pin data in that channel reveal, there is a substantial load on the banks that can not be attributed to streamflow and therefore points to boating activities. The greater ratio of boat to streamflow loading in these very small channels may result in a discernible physical impact.

Bibliography

ADNR 2002 Chilkat bald eagle preserve management plan: public review draft. *Tech. Rep.*. Alaska Department of Natural Resources.

Arruda, J., Marzolf, G. & Faulk, R. 1983 The role of suspended sediments in the nutrition of zooplankton in turbid reservoirs. *Ecology* **64** (5), 1225–1235.

Bash, J., Berman, C. & Bolton, S. 2001 Effects of turbidity and suspended solids on salmonids. *Tech. Rep.*. Center for Streamside Studies, University of Washington.

Berg, L. 1982 The effect of exposure to short-term pulses of suspended sediment on the behavior of juvenile salmonids. In *Proceedings of the Carnation Creek Workshop: a ten-year review* (ed. G. Hartman), pp. 177–196. Department of Fisheries and Oceans, Pacific Biological Station.

Berg, L. & Northcote, T. 1985 Changes in territorial, gill-flaring, and feeding behavior in juvenile coho salmon following short-term pulses of suspended sediment. *Canadian Journal of Fisheries and Aquatic Sciences* **42**, 1410–1417.

Breitburg, D. 1988 Effects of turbidity on prey consumption by striped bass larvae. *Transactions of the American Fisheries Society* **117**, 72–77.

Bugliosi, E. 1985 Hydrologic reconnaissance of the Chilkat River basin, southeast Alaska. *Tech. Rep.* 84-618. United States Geological Survey.

Gregg, R. & Bergersen, E. 1980 *Mysis relicta*: effects of turbidity and turbulence on short-term survival. *Transactions of the American Fisheries Society* **109**, 207–212.

Hill, D., Beachler, M. & Johnson, P. 2002 Hydrodynamic impacts of commercial jet boating on the Chilkat River, Alaska. *Tech. Rep.*. The Pennsylvania State University, prepared for the Alaska Department of Fish and Game.

Killgore, K., Miller, A. & Conley, K. 1987 Effects of turbulence on yolk-sac larvae of paddlefish. *Transactions of the American Fisheries Society* **116**, 670–673.

Morgan, R., Rasin, V. & Noe, L. 1983 Sediment effects on eggs and larvae of striped bass and white perch. *Transactions of the American Fisheries Society* **112**, 220–224.

Morgan, R., Ulanowicz, R., Jr. V. R., Noe, L. & Gray, G. 1976 Effects of shear on eggs and larvae of striped bass, *Morone Saxatilis*, and white perch, *M. Americana*. *Transactions of the American Fisheries Society* **106**, 149–154.

Neitzel, D., Abernethy, C. & Richmond, M. 1998 Laboratory studies of the effects of turbulence and shear stresses on turbine-passed fish. Progress report. Pacific Northwest National Laboratory, Richland, WA, 99352.

Newcombe, C. & MacDonald, D. 1991 Effects of suspended sediments on aquatic ecosystems. *North American Journal of Fisheries Management* **11**, 72–82.

Rehmann, C., Stoeckel, J. & Schneider, D. 2003 Effect of turbulence on the mortality of zebra mussel veligers. *Canadian Journal of Zoology* **81**, 1063–1069.

Rutherford, J. 1994 *River Mixing*. John Wiley and Sons.

Servizi, J. & Martens, D. 1987 Some effects of suspended Fraser River sediments on sockeye salmon (Oncorhynchus nerka). In *Sockeye salmon population biology and future management* (ed. H. Smith, L. Margolis & C. Wood), , vol. 96, pp. 254–264. Canadian Special Publication of Fisheries and Aquatic Sciences.

Sigler, J., Bjornn, T. & Everest, F. 1984 Effects of chronic turbidity on density and growth of steelheads and coho salmon. *Transactions of the American Fisheries Society* **113**, 142–150.

Sutherland, A. & Ogle, D. 1975 Effect of jet boats on salmon eggs. *New Zealand Journal of Marine and Freshwater Research* **9** (3), 273–282.